Morphological Operators on the Unit Circle

Allan G. Hanbury and Jean Serra

Abstract—Images encoding angular information are common in image analysis. Examples include the hue band of color images, or images encoding directional texture information. Applying mathematical morphology to image data distributed on the unit circle is not immediately possible, as the unit circle is not a lattice. Three approaches to solving this problem are presented. First, difference-based operators are studied (e.g., gradient, top-hat). Second, a definition of grouped circular data is suggested, and "pseudo" morphological operators, which operate only on grouped data, are introduced. Finally, processing using pixel labeling is presented, leading to the development of a cyclic opening operator. Applications for treating the hue band of color images and for finding perturbations in wood texture are given.

Index Terms—Angular data, color image analysis, morphological operation, oriented texture analysis, rotational invariance.

I. INTRODUCTION

IN IMAGE analysis, one often has to treat data distributed on the unit circle. The two studies which motivated the development of the theoretical elements presented in this paper illustrate some situations which are often encountered. The first one involves the description of directional textures; the second one involves the filtration of the hue component of color images.

The application of morphological operators to the hue band of color images is related to another subject which has received much attention, namely, morphology for vector images, specifically color images. A number of possible orders for color vectors in the RGB color space have been proposed [1]–[4]. Work using an angular representation of hue, and hence more closely related to the approach presented in this paper, is presented by Peters [5], who develops morphological operators on the hue circle which require the choice of an origin; Demarty and Beucher [6] who treat image segmentation in the HLS color space; and Zhang and Wang [7] who present definitions of two distances on the hue circle in the context of color image segmentation.

The unit circle, like the round table of King Arthur's knights, has no order of importance, and no dominant position. In mathematical terms, this signifies that we cannot construct a lattice on the unit circle unless we assign it an arbitrary origin. This is a severe verdict against morphological treatments (i.e., operators relying on lattices) when we use them on the unit circle.

However, is it really impossible to bypass this interdiction? If we consider the standard morphological operators, three paths

seem possible. First, there is the class of operators which bring into play a difference, such as gradients, top-hats, medians, etc. Does this difference not introduce a local origin, obviously variable at each point, but sufficient to transfer to the circular case? Section II treats these operators.

The second approach, covered in Section III, considers the grouping of circular data. Deciding on the number of groups in a dataset is not straightforward, so we introduce a simple criterion for grouped data, and define the basic morphological operators so that they act only if a structuring element contains grouped data.

The third approach, developed in Section IV, involves a different way of viewing the situation. A sequence of labels with index $i \in \mathbb{N}$ defined on the unit circle can serve to index the angles. On the hue circle, there could be a royal blue class, an apple green class, etc., with the condition that the labels with numbers $i + N$ are identical to those numbered i. If every pixel in the image is assigned a label, then we have an indexed partition of the image. With two labels, one is in a situation analogous to that of a binary image. For this case, the alternating filters of type $\varphi\gamma$ (i.e., the result of a composition of an opening by a closing) can also be viewed as the product of two openings operating successively on the two labeled regions "foreground" and "background." If, instead of two labels, we have N, and if we perform a cycle of N openings successively on each of the labeled regions, what is the result?

II. CIRCULAR CENTERED OPERATORS

We fix an origin a_0 on the unit circle C with center o by, for example, choosing the topmost point, and indicate the points a_i on the circle by their curvilinear coordinate in the trigonometric sense between 0 and 2π from a_0. Given two points a and a', we use the notation $a \div a'$ to indicate the value of the acute angle aoa', i.e.

$$a \div a' = \begin{cases} |a - a'|, & \text{if } |a - a'| \leq \pi \\ 2\pi - |a - a'|, & \text{if } |a - a'| \geq \pi. \end{cases} \quad (1)$$

If the a_i are digital values between 0 and 255 (for example), the expression "$\leq \pi$" becomes "≤ 127," and "2π" becomes "255." However, we continue using the notation in terms of π, as it is more enlightening. In [5], (1) appears applied to the treatment of the hue band of color images.

A. Gradient

In the Euclidean space $\mathbb{R}^d$, to determine the modulus of the gradient at point x of a numerical differentiable function f, one considers a small sphere $S(x, r)$ centered on x with radius r.

Then, one takes the supremum minus the infimum of the increments $|f(x)-f(y)|$, where y describes the small sphere $S(x,r)$, i.e.

$$g(x, r) = \{\vee[|f(x) - f(y)|, y \in S(x, r)] \\ - \wedge [|f(x) - f(y)|, y \in S(x, r)]\}/2r. \quad (2)$$

Finally, one determines the limit of the function $g(x, r)$ as r tends to zero. This limit exists as the function f is differentiable in x. In the two-dimensional (2-D) digital case, it is sufficient to apply (2), taking for $S(x, r)$ the unit circle centered on x (square or hexagon). This is the classic Beucher algorithm [8] for the gradient.

Consider now an image of hues or of directions, i.e., a function $a\colon E \to C$, where E is an Euclidean or digital space and C is the unit circle. As the gradient calculation involves only increments, we can transpose (2) to the circular function a by replacing all the $|f(x) - f(y)|$ by $[a(x) \div a(y)]$. This transposition then defines the modulus of the gradient of the circular distribution. For example, in a digital space $\mathbb{Z}^d$, $K(x)$ indicates the set of neighbors at distance one from point x, hence

$$(\operatorname{grad} a)(x) = \tfrac{1}{2} \vee \{[a(x) \div a(y)], y \in K(x)\} \\ - \tfrac{1}{2} \wedge \{[a(x) \div a(y)], y \in K(x)\}. \quad (3)$$

As an illustration, consider the hue component of Fig. 1(a), shown in Fig. 2(a). This image was chosen as it is mostly red in color, and in the angular hue encoding, red usually has hue values around $0°$. This means that pixels which appear red could have low hue values (e.g., $0°$–$30°$) and high hue values ($330°$–$360°$). A large discontinuity is therefore visible in the hue image, with red pixels appearing at the extremities of the histogram [Fig. 2(b)]. A classical gradient on this hue band produces a large number of spurious high-valued pixels, as shown in Fig. 2(c). These high values are present even though the neighboring pixels appear very similar in color, and are due to the discontinuity in the hue encoding. A good illustration of this is the outer part of the halo, which appears smooth in Fig. 1(a), but results in very high gradients in Fig. 2(c). The gradient calculated using (3), shown in Fig. 2(d), overcomes this problem. Note that for this example, if we rotate the hue band pixel values by π, the classical gradient will be the same as the circular centered gradient. The circular centered gradient is, however, invariant to rotations of the pixel values.

B. Top-Hat

The notion of the "top-hat," in the sense of F. Meyer [8], is the residue between a numerical function and its transformation by an opening. It therefore involves only increments, and hence can be transposed to functions of values in C. We explain below the algorithm for the use of openings by adjunction (i.e., products by composition of an erosion by the adjunct dilation). We begin by reminding the reader of the relation which gives the value $\gamma_B(x)$ of the opening by the structuring element B, at point x. If we indicate by $\{B_i, i \in I\}$ the family of structuring elements which contain point x

$$\gamma_B(x) = \sup\{\inf[f(y), y \in B_i], i \in I\}.$$

(a)

(b)

Fig. 1. Images used in the examples. The original color images are available on the world wide web at http://cmm.ensmp.fr/~hanbury/morph_unit_circle/.

For the top-hat $f(x) - \gamma_B(x)$ we therefore write

$$f(x) - \gamma_B(x) = - \sup\{\inf[f(y) - f(x), y \in B_i], i \in I\} \quad (4)$$

in which there are only increments of the function f around point x. We can therefore transpose to functions of circular values a exactly as we did for the gradient, and give the definition

$$(\text{top-hat})(x) = - \sup\{\inf[-(a(x) \div a(y)), y \in B_i], i \in I\}. \quad (5)$$

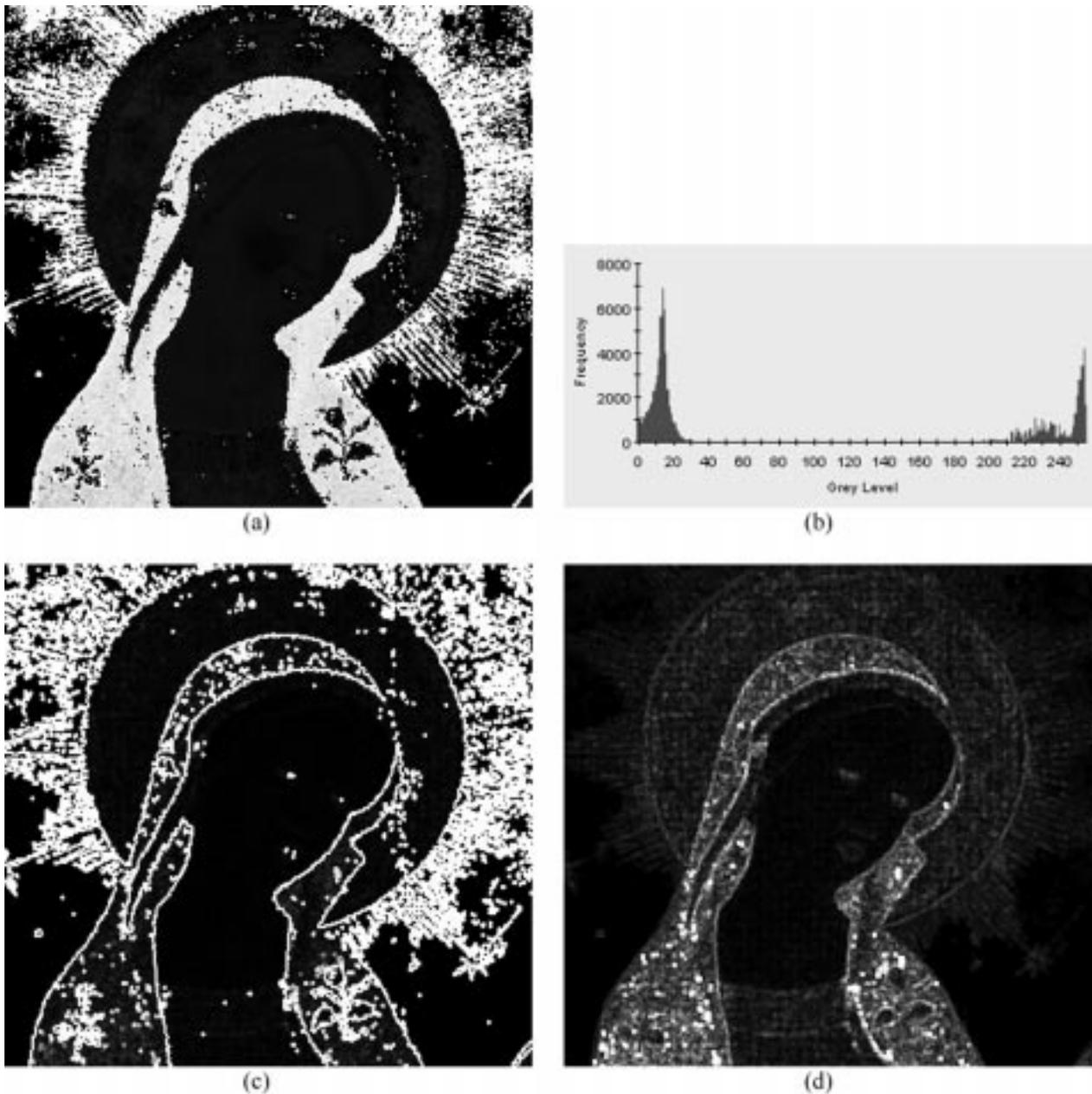An example of a top-hat of this type is given in Fig. 3. Fig. 3(a)

Fig. 2.   (a) Hue band of the virgin image in Fig. 1(a) (image size 352×334 pixels). (b) Histogram of the hue band. (c) Classical morphological gradient on the hue band. (d) Circular centered (angular) gradient on the hue band. The gradients were calculated using a 3×3 structuring element.

is a subsection of the luminance band of Fig. 1(b) which contains some regions (indicated by the white rectangles) in which the dominant color is red, that is, they fall on the hue discontinuity, as is seen in the corresponding regions in the hue image [Fig. 3(b)]. A classical white top-hat (4) applied to the hue band is shown in Fig. 3(c), with its histogram in Fig. 3(e). Once again, it is evident that even though there is not much visible change in the color within the indicated regions, there are many high-valued pixels in the result of the top-hat transformation. This is further demonstrated by the relatively large number of pixels near the upper end ($360°$) of the histogram. The result of applying the circular centered top-hat (5) is shown in Fig. 3(d), with its histogram in Fig. 3(f). In this image, the spurious high-valued pixels do not appear.

An alternative formulation of the top-hat is given in Section IV.

III. PSEUDO-OPERATORS

The main shortcoming of the unit circle morphological operators proposed in [5] is the requirement to choose an origin, which in some cases would lead to the user having to make an arbitrary choice. In this section, we propose an alternative formulation, where one is not required to choose an origin, but instead must provide a definition of grouped circular data. We introduce a possible definition of grouped data in the framework of the morphological center, and then extend this definition to the erosion and dilation operators.
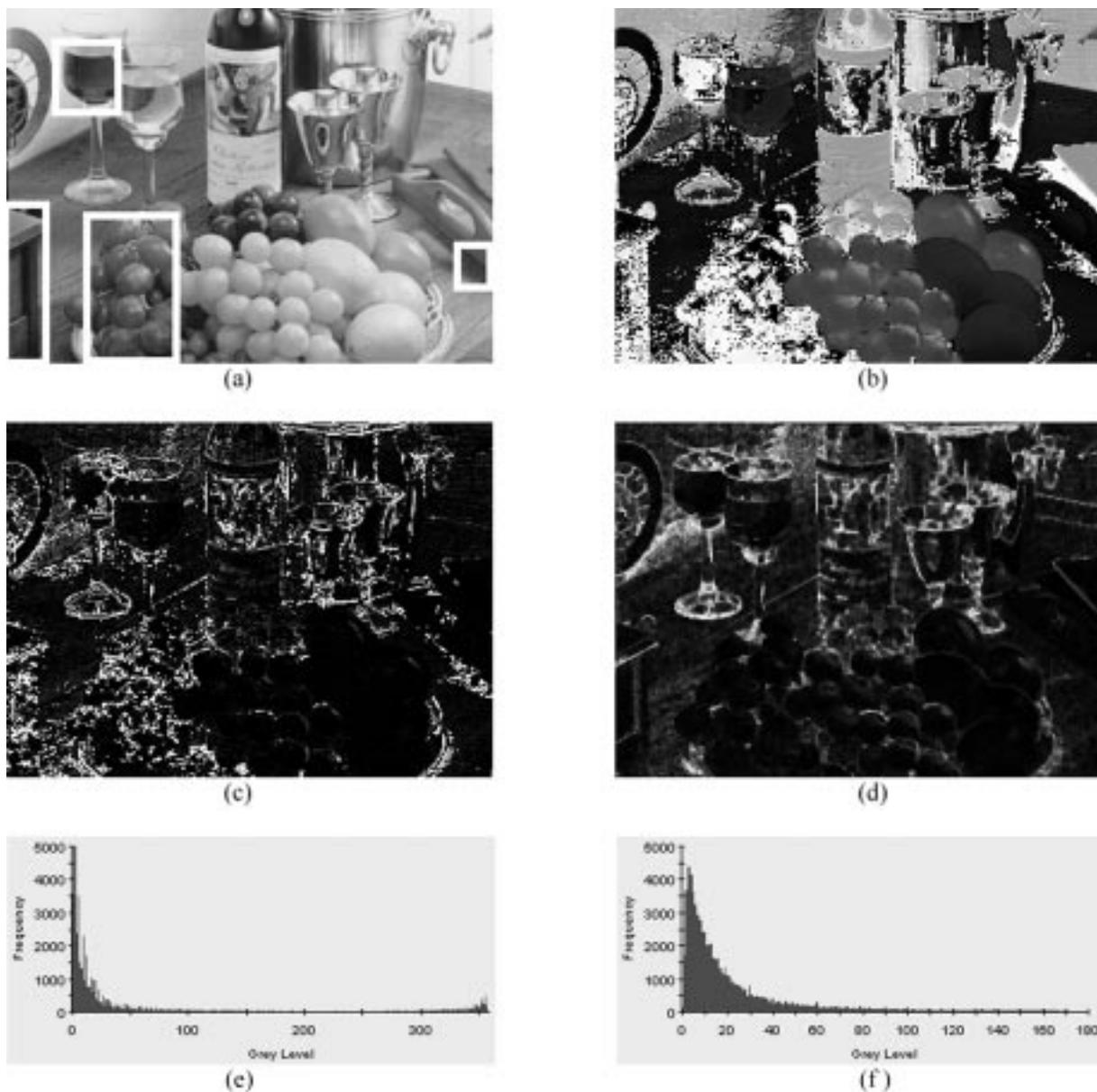
Fig. 3. (a) Subsection of Fig. 1(b) with the red parts indicated (image size 311×227 pixels). (b) Hue band of image a. (c) Classic white top-hat with a 3×3 square of image a. (d) Circular centered top-hat with a 3×3 square of image a. (e) Histogram of image c. (f) Histogram of image d.

A. Morphological Center

The morphological center is a notion which naturally appears in the self-dual morphological filters [9]. Consider n numerical values $t_i \in \mathbb{R}$ and a number t which we wish to bring closer to the t_i. The "morphological center" operator κ acts as follows:

$$\kappa(t) = \begin{cases} \wedge t_i, & \text{if } t \leq \wedge t_i \\ t, & \text{if } \wedge t_i \leq t \leq \vee t_i \\ \vee t_i, & \text{if } \vee t_i \leq t. \end{cases} \qquad (6)$$

In particular, for $n = 2$ we find the median between three values: t_1, t_2, and t. The identification can be expanded by iteration to $n > 2$. However, we limit ourselves to transposing (6) to circular data.

Nonetheless, a difficulty is apparent. On the line, we can always say whether a value t is exterior (superior or inferior) to t_i.

On the circle, we can make sense of this expression in the case of distributions such as those in Fig. 4(a)–(c), but not in Fig. 4(d), where the data are too dispersed. We describe two possible approaches, and develop the second one further.

1) We replace a unconditionally by the closest a_i, by applying

$$\kappa_0(a) = \{a_i | (a_i \div a) = \wedge(a_i \div a), i \in I\}.$$

2) Alternatively, we construct conditions similar to those in (6). It therefore becomes necessary to formally define the notion of a group of points, of which Fig. 4(a)–(c) give an intuitive idea. We adopt the notion that the points are grouped if they are spread over a segment smaller than a semi-circle, or, stated formally.
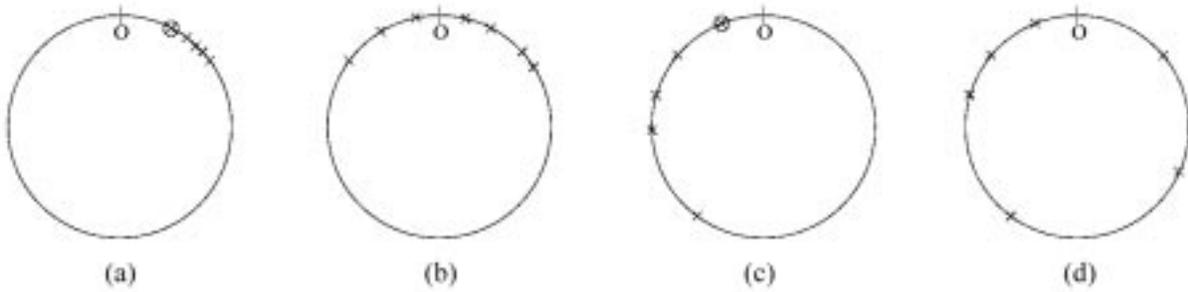
Fig. 4. Four distributions of circular data. (a), (b), and (c) are ω-grouped; (d) is not.

Definition: A family $\{a_i, i \in I\}$ of points on a unit circle is ω-grouped when there exists an origin such that

$$(\vee a_i, \, i \in I) - (\wedge a_i, \, i \in I) \leq \omega \leq \pi \qquad (7)$$

where ω is an angle less than or equal to π.

The condition $\omega \leq \pi$ suppresses the case shown in Fig. 4(d). The following proposition characterizes the groups of points using their coordinates.

Proposition: The family $\{a_i, i \in I\}$ of the points on the unit circle C forms an ω-group if and only if one has

$$\vee\{a_i, i \in I\} - \wedge\{a_i, i \in I\} \leq \omega \qquad (8)$$

for an arbitrary origin a_0, or for the origin $a_0 + \pi$.

Proof: If the a_i are ω-grouped, there exists a partition of C into two semi-circles so that all the a_i are found in one of the semi-circles. If we take for a_0 some point in the opposite semi-circle, (8) is verified, because a_0 does not belong to the envelope of the group of points (i.e., to the smallest sector of the circle which contains them all). Conversely, if (8) is satisfied for an origin a_0, it is sufficient to move this origin to the point $\wedge\{a_i, i \in I\}$ to get (7), the definition of an ω-group of the a_i.

The algorithm defining the circular morphological center develops directly from the preceding proposition. It is sufficient to take as the origin the point a that we wish to compare to the family $\{a_i\}$. We simply remember that, as we must use positive coordinates, the differences implicit in a change of origin are written thus

$$\mathrm{dif}(a_i, a) = \begin{cases} a_i - a, & \text{if } a_i - a \geq 0 \\ 2\pi + a_i - a, & \text{otherwise.} \end{cases}$$

Definition: Given a family $\{a_i, i \in I\}$ and a point on the unit circle, and hence a grouping angle ω, the transformation $\kappa(a)$ of a by morphological centering is defined as

$$\kappa(a) = \begin{cases} a, & \text{if } \alpha \geq \pi \\ \wedge a_i, & \text{if } \alpha \leq \pi \text{ and } (a \div \wedge\{a_i, i \in I\}) \\ & \qquad < (a \div \vee\{a_i, i \in I\}) \\ \vee a_i, & \text{if } \alpha \leq \pi \text{ and } (a \div \vee\{a_i, i \in I\}) \\ & \qquad < (a \div \wedge\{a_i, i \in I\}) \end{cases}$$

with $\alpha = \vee\{\mathrm{dif}(a, a_i), i \in I\} - \wedge\{\mathrm{dif}(a, a_i), i \in I\}$.

In other words, if there is an ω-group and a is outside the group ($\alpha \leq \pi$), one replaces a by the extremity of the group closest to a. If there is no grouping, or if a is inside the ω-group of the a_i ($\alpha \geq \pi$ for both these cases), one leaves it unchanged.

In the case of Fig. 4, if we take the origin as the point to transform, it does not change for Fig. 4(b) and (d), and becomes the circled point in Fig. 4(a) and (c). In [10], a similar subject, the color median filter operating on three-dimensional color vectors in the RGB space, is treated.

B. Erosion and Dilation

The notion of an ω-group (7) suggests the introduction of two operators which approximate a supremum and an infimum. Consider a finite ω-group $\{a_i, i \in I\}$. For all the origins for which (8) is valid, the number $a_{\max} = \vee\{a_i, i \in I\}$, even though its numerical value depends on the position of the origin, always corresponds to the same point of the group. The same applies to the infimum $\wedge\{a_i, i \in I\}$. These two extremities therefore have a significance partially independent of the choice of the origin on the unit circle.

This observation leads naturally to the introduction of a "pseudo-dilation" operator. Consider a function $a : E \to C$, i.e., for every point x in the space E, $a(x)$ is a value on the unit circle, and let $B(x)$ be a structuring element, i.e., an arbitrary function $B : E \to \mathcal{P}(E)$, where $\mathcal{P}(E)$ represents the set of the subsets of E. The pseudo-dilation $\delta : C^E \to C^E$ is defined as

$$(\delta(a))(x) = \begin{cases} \vee\{a_i(y), y \in B(x)\}, & \text{if } \{a_i(y), y \in B(x)\} \\ & \qquad \text{forms an } \omega\text{-group} \\ a(x), & \text{otherwise.} \end{cases}$$

The operator δ certainly depends on the choice of the origin but, by construction, commutes with the rotations on the unit circle (i.e., with changes of the origin). It is not a dilation, as one cannot find an underlying order relation, and not, a fortiori, a lattice. Nevertheless, for all symmetric B we can define, by duality, a "pseudo-erosion"

$$(\epsilon(a))(x) = \begin{cases} \wedge\{a_i(y), y \in B(x)\}, & \text{if } \{a_i(y), y \in B(x)\} \\ & \qquad \text{forms an } \omega\text{-group} \\ a(x), & \text{otherwise.} \end{cases}$$

It follows that all the classic extensive operators in mathematical morphology, such as openings, closings, reconstruction, leveling, etc., have a "pseudo" version.

Fig. 5 provides a comparison between the pseudo-erosion and standard erosion. Fig. 5(a) is the hue band of a subsection of Fig. 1(b). Fig. 5(b) shows a pseudo-erosion and Fig. 5(c), a standard erosion of this hue band. The region in which the differences are most pronounced is for the red fruit to the left of the image. The hue values for red straddle the discontinuity at
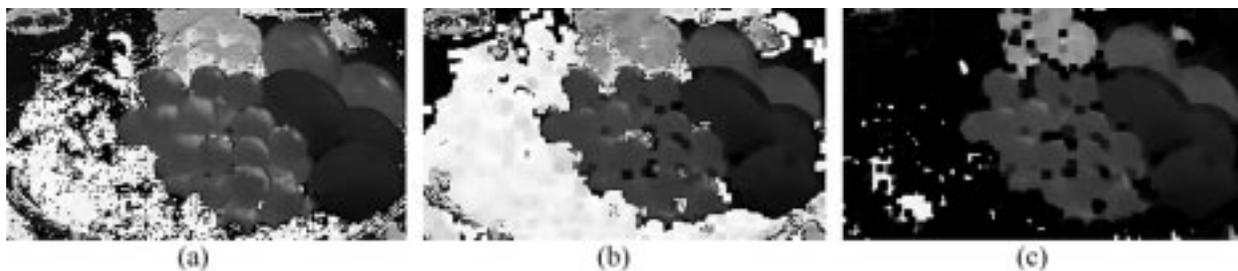
Fig. 5.   (a) Hue band of a subsection of Fig. 1(a) (image size 231×134 pixels). (b) Pseudo-erosion of image a. (c) Standard erosion of image a. Both erosions are by a 5×5 pixel square.

$0°/360°$, and the standard erosion reduces these to small values greater than zero. The pseudo-erosion, however, replaces the pixels with the infimum of the group of values around $0°$. One should notice the regions, such as the base of the wine glass, where this erosion operator does not change the pixel values as they do not form an ω-group.

In introducing these pseudo-operators, in order to avoid the necessity of choosing an origin, one unfortunately loses a number of desirable properties of standard morphological operators. One example is that the pseudo-opening and pseudo-closing operators are not idempotent (but are usually idempotent after a few iterations). This lack of idempotence is due to the pseudo-operators not acting in the same way on all pixels, but leaving some pixels in their original states. The decision as to whether to leave a pixel or change it depends on the distribution of the values of the pixels in the structuring element, and this distribution changes after each application of an operator.

IV. Labeled Openings

Circular data may be treated in another manner, which is more set oriented, and where there is no obligation to define groups or work on increments. This third approach is based on the idea of first labeling the points of the working space according to the local hue or angle, then processing the obtained sets, and finally combining the results in an isotropic way.

A. Theory

Denote by $A(\alpha, \omega)$ the set of those points $x \in E$ whose angular value $a(x)$ lies in acute sector $[\alpha, \alpha + \omega]$

$$A(\alpha, \omega) = \{x: x \in E, a(x) \in [\alpha, \alpha + \omega]\}.$$

Now let $\{\gamma_\lambda, \lambda > 0\}$ be an opening of size λ on $\mathcal{P}(E)$. The opening $\gamma_\lambda A(\alpha, \omega)$ is performed as for a binary opening, with $A(\alpha, \omega)$ treated as the foreground, and the rest as the background. In order to isotropize this operation, we take the union of all transforms $\gamma_\lambda[A(\alpha, \omega)]$ as α traces out the unit circle, i.e.,

$$\underline{\gamma}(\lambda, \omega) = \cup\{\gamma_\lambda[A(\alpha, \omega)], 0 \leq \alpha \leq 2\pi\}. \qquad (9)$$

The result is a binary image containing as foreground all the pixels which are not removed by the action of the opening for one of the angles α. The residue (in the sense of the top-hat) of this opening is obtained by inverting $\underline{\gamma}(\lambda, \omega)$, that is

$$\underline{R}_\gamma(\lambda, \omega) = \overline{\underline{\gamma}(\lambda, \omega)}. \qquad (10)$$

The residue consists of the pixels which were eliminated by the opening for all angles α.

When the angle ω varies from 0 to π, it is clear that the opening $\underline{\gamma}$ is an increasing function of ω. As usual, this opening is also a decreasing function of the size parameter λ. These considerations lead to the following proposition.

Proposition: Let $a: E \to C$ be a function of circular values, γ_λ a granulometry on $\mathcal{P}(E)$, and $A(\alpha, \omega): \mathcal{P}(E) \to \mathcal{P}(E)$ the angular restriction

$$A(\alpha, \omega) = \{x: x \in E, a(x) \in [\alpha, \alpha + \omega]\}.$$

Then the operator

$$\underline{\gamma}(\lambda, \omega) = \cup\{\gamma_\lambda[A(\alpha, \omega)], 0 \leq \alpha \leq 2\pi\}$$

is an isotropic opening. The family $\{\underline{\gamma}(\lambda, \pi - \omega), 0 \leq \omega \leq \pi, \lambda > 0\}$ engenders a *double granulometry* with respect to the two parameters λ and $\pi - \omega$.

In practice, ω expresses the amount of variation permitted in the angles constituting a region. The above labeled openings treat the data in a parallel way (e.g., each $\gamma_\lambda[A(\alpha, \omega)]$ could be performed by an independent processor).

B. Application

An industrial application of the labeled opening is presented. When sorting oak boards destined to be used to make furniture, it is necessary to find the knots, and to measure the sizes of the small light patches. These two characteristics have been highlighted in Fig. 6(a), where the knots are surrounded by black rectangles and the light patches by white rectangles (the three light horizontal lines in this image are chalk lines drawn on the board and are of no importance). Knots can be found using color and texture characteristics, as they are usually much darker than the surrounding wood, and usually perturb the directions of the surrounding veins. The light patches are generally of a similar color to other parts of the wood, but tend to cut veins, causing a disruption in the dominant local texture orientation. An application of the labeled opening operator to finding regions of anomalous texture orientation is presented here.

Wood texture is oriented, meaning that there is a dominant orientation in the neighborhood of each image point. This texture can therefore be represented by an image encoding the dominant orientation in each pixel neighborhood. An algorithm based on that developed by Rao [11] is used to extract these orientations. The steps in this algorithm are as follows.
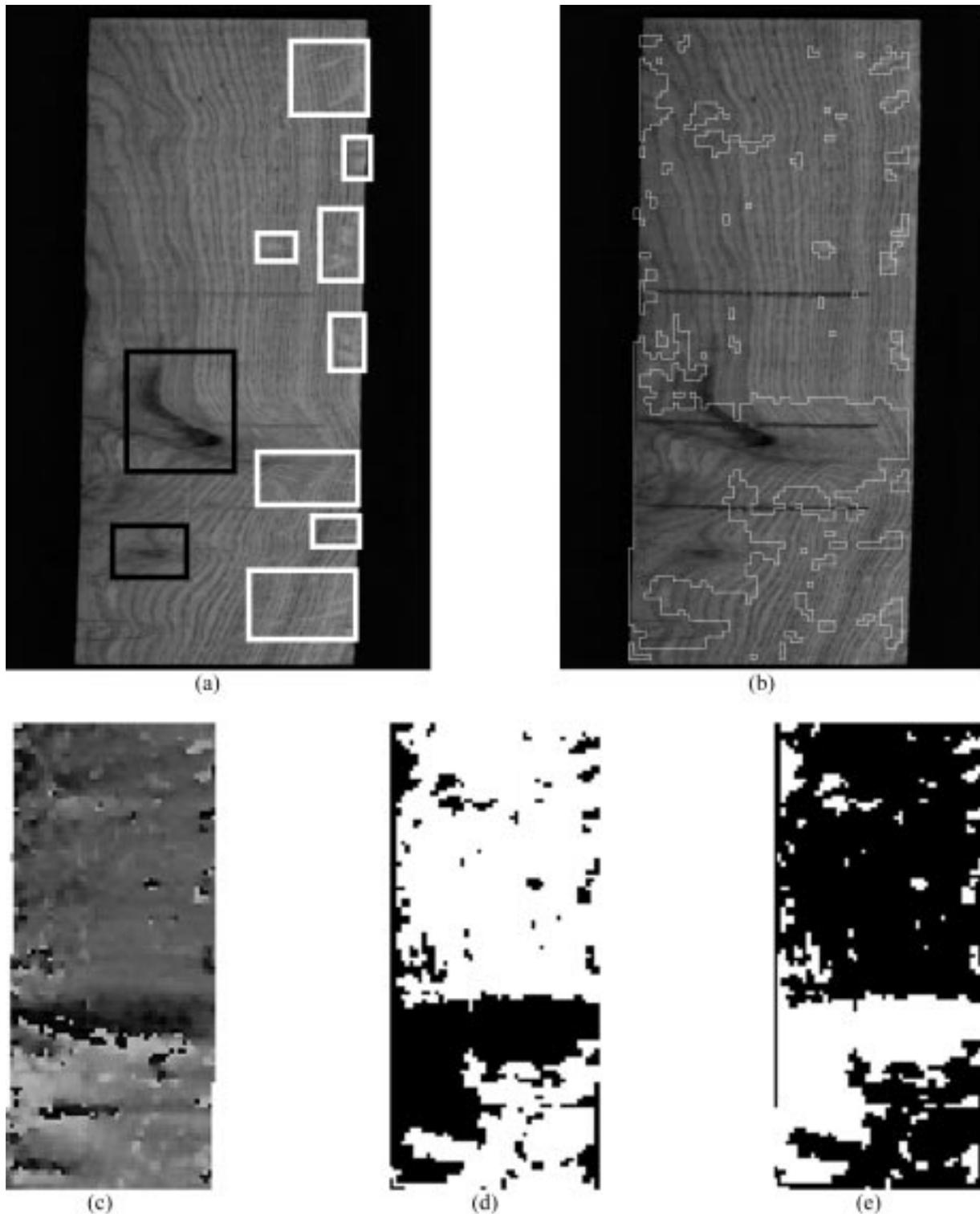
Fig. 6. (a) Oak board with knots (indicated by black rectangles) and light patches (indicated by white rectangles) (image size 608×955 pixels). (b) Residue of the labeled opening on the orientation image expanded and projected onto the original image (the regions enclosed by the white outlines correspond to the residue). (c) Reduced orientation image (size 50×112 pixels) calculated using the Rao algorithm. (d) Union of the opening of each labeled region. (e) Residue of the labeled opening on the orientation image.

Step 1) Detection of the edges of the wood and cropping of the image to contain only the wood.

Step 2) Convolution by a Gaussian filter of size 5×5 with Gaussian width $\sigma = 1.4$.

Step 3) Calculation of the angle at every pixel in the image from the horizontal and vertical gradients.

Step 4) Determination of the dominant angle within a moving frame of size 16×16 pixels, moved in steps of eight pixels horizontally and vertically.

Step 5) Construction of the reduced size orientation image which encodes the dominant orientation in each frame by a single pixel.
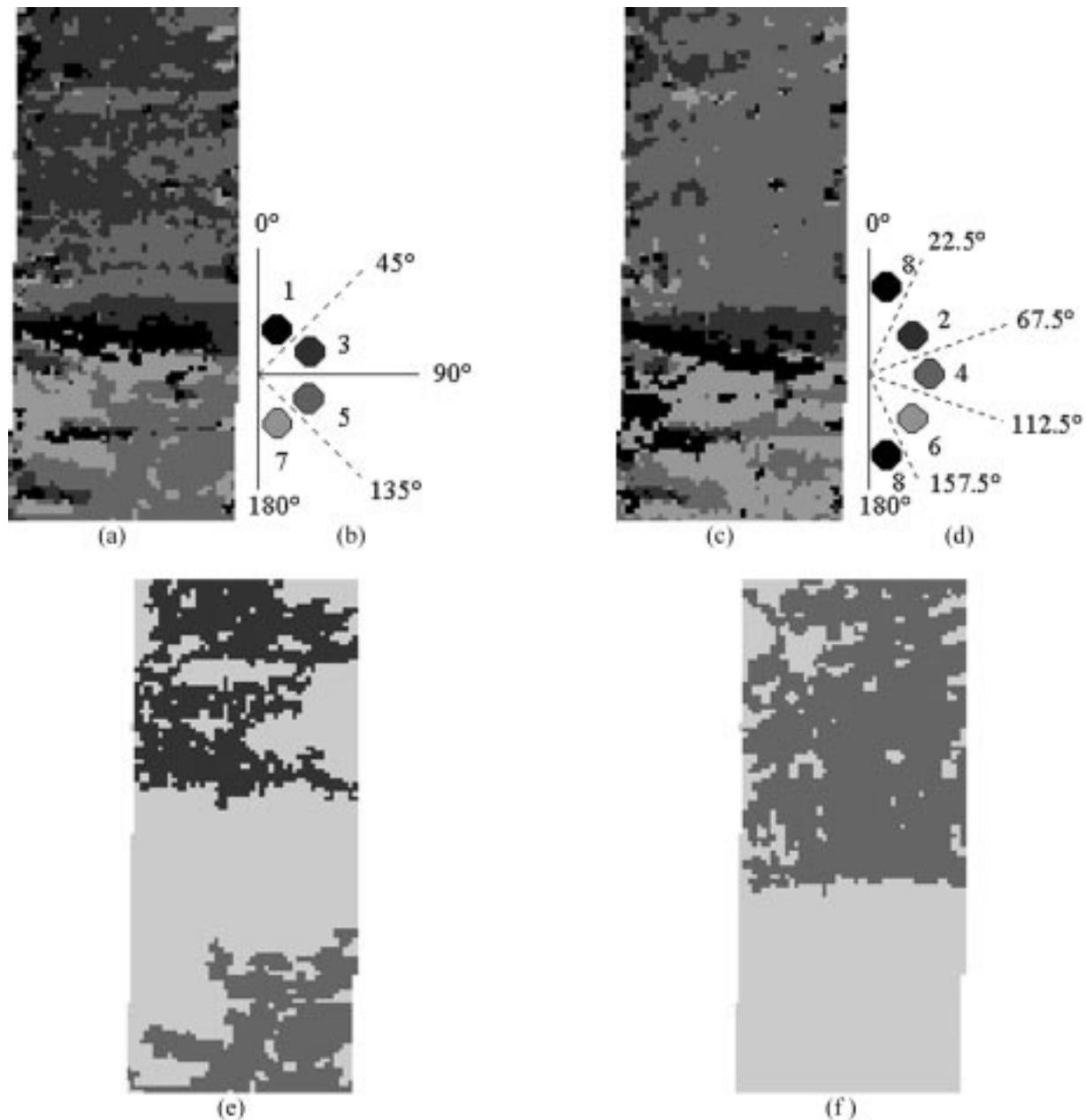
Fig. 7. (a) and (c): The labels defined on the orientation image [Fig. 6(c)]. (b) and (d): the label definitions. (e): the connected opening by a square of size nine pixels of each label shown in image a (the lightest grey represents the labeled regions eliminated by the opening). (f): the same opening performed on image c.

As the orientation of a vein can equally well be described by two directions, namely, θ and $\theta + 180°$, the angles are restricted to values between $0°$ and $180°$, such that $\theta + 180° = \theta$. The reduced size orientation image for Fig. 6(a) is shown in Fig. 6(c).

The aim is for the regions of anomalous orientation to appear as the residue of a labeled opening. We used a connected labeled opening (opening with reconstruction) with $\omega = 45°$ and a square structuring element with side of length nine pixels. The isotropization of the opening (9) was approximated by varying α from $0°$ to $157.5°$ in steps of $22.5°$. The resulting label definitions are shown in Fig. 7(b) and (d), and the corresponding labeled images in Fig. 7(a) and (c) (two labeled images are shown as the angular values of the labels overlap). The numbers shown on the label definition diagrams indicate the order of the labeling as the value of α increases. The result of the opening on

each of the labels in Fig. 7(a) and (c) are shown, respectively, in Fig. 7(e) and (f), where the lightest grey represents the regions eliminated by the opening operator. The union of the labeled regions not eliminated by the opening (10) is shown in Fig. 6(d). The residue [the inverse of Fig. 6(d)] is shown in Fig. 6(e), and this residue expanded and projected onto the original image is shown in Fig. 6(b), where the regions enclosed by the white outlines correspond to the residue.

The region of severe perturbation of veins due to the knots on the lower part of the wood is found, although the upper part of the largest knot is not detected as it is parallel to the veins forming the largely homogeneous upper region of the board. Most of the light patches are also detected. There are a few false detections, corresponding to regions where there is a change in the orientation of the veins without an associated defect (for

example, at the top left of board), or to tiny misdetections which could be eliminated by a subsequent area opening.

This algorithm has been applied to a database of 60 oak images with good results. However, even though defects are associated with texture orientation perturbations, the presence of such a perturbation does not guarantee the presence of a defect. The results of this transform should therefore ideally be used as input to a decision procedure, which uses color and further texture information to calculate the likelihood of a defect being present.

V. CONCLUSION

Three possible approaches to applying mathematical morphology to circular data are presented. The first involves using differences (increments), the second makes use of a definition for grouped circular data, and the third uses labels. Difference versions of the gradient and top-hat are presented. Second, a formulation of "pseudo" versions of the erosion and dilation operators are given, which can be expanded to create the other standard morphological operators. They have the advantage of not requiring the choice of an origin on the circle, but suffer from some unfortunate properties such as the non-idempotence of the pseudo-opening and pseudo-closing operators. Finally, openings on labeled images are presented. Applications of these operators to the hue band of color images and to images encoding directional texture information are given. In addition to these applications, these operators could be applied to any images containing phase information, such as electron microscope images or spectrograms. In practice, we find that the use, if possible, of the circular centered operators or labeled operators give the best results.

The reader should be aware that in most cases, circular data does not appear alone, but is combined with other non-circular values. For color images, these are usually luminance or intensity and saturation; and for oriented textures, measures of magnitude or coherence. More generally, the question arises with vector data when one wants their processing to be independent of the choice of the vector base. For example, a 2-D Euclidean vector (x, y) may be represented in polar coordinates (ρ, θ). Then any processing that combines the above circular operators (for θ) with operators on ρ yields a result that does not depend on the orientation of the initial base (x, y). A similar comment applies in $\mathbb{R}^3$ when vectors are decomposed into their spherical or their cylindrical representations. The development of operators which treat these non-angular values along with the related angular quantities in a rotationally invariant way is an interesting topic for further development.

Finally, we note that a detailed experimental comparison of the angular morphological operators with standard operators on the same data set is not done, as it is immediately obvious from the data which approach should be used. If, during the analysis of a set of data or an image, one has to choose an arbitrary origin before applying an operator, then the rotationally invariant operators in this paper are to be preferred.

REFERENCES

[1] J. Chanussot and P. Lambert, "Total ordering based on space filling curves for multivalued morphology," in *Proc. ISMM*, 1998, pp. 51–58.

[2] M. L. Comer and E. J. Delp, "Morphological operations for color image processing," *J. Electron. Imag.*, vol. 8, pp. 279–289, July 1999.

[3] M. C. d'Ornellas, R. Boomgaard, and J. Geusebroek, "Morphological algorithms for color images based on a generic-programming approach," in *Proceedings of the XI Brazilian Symposium on Computer Graphics and Image Processing (SIBGRAPI'98)*.   Piscataway, NJ: IEEE Press, 1998.

[4] H. Talbot, C. Evans, and R. Jones, "Complete ordering and multivariate mathematical morphology: Algorithms and applications," in *Proc. ISMM*, 1998, pp. 27–34.

[5] R. A. Peters, II, "Mathematical morphology for angle-valued images," *Proc. SPIE*, vol. 3026, 1997.

[6] C.-H. Demarty and S. Beucher, "Color segmentation algorithm using an HLS transformation," in *Proc. ISMM*, 1998, pp. 231–238.

[7] C. Zhang and P. Wang, "A new method of color image segmentation based on intensity and hue clustering," in *Proc. 15th ICPR*, vol. 3, Barcelona, Spain, 2000, pp. 617–620.

[8] J. Serra, *Image Analysis and Mathematical Morphology*.   New York: Academic, 1982.

[9] ——, *Image Analysis and Mathematical Morphology Volume 2: Theoretical Advances*.   New York: Academic, 1988.

[10] P. E. Trahanias, D. Karakos, and A. N. Venetsanopoulos, "Directional processing of color images: Theory and experimental results," *IEEE Trans. Image Processing*, vol. 5, pp. 868–880, June 1996.

[11] A. R. Rao, *A Taxonomy for Texture Description and Identification*.   New York: Springer-Verlag, 1990.

Allan G. Hanbury was born in George, South Africa, in 1974. He received the B.Sc.(Hons.) and M.Sc. degrees in physics from the University of Cape Town, South Africa, in 1995 and 1999, respectively. He is presently pursuing the Ph.D. degree at the Centre of Mathematical Morphology, Paris School of Mines, France.

He is presently a Researcher at the Centre of Mathematical Morphology, Paris School of Mines. His main topics of research are the application of mathematical morphology to images encoding directional information, defect detection in textures, and the development of algorithms for real-time wood inspection applications.

Jean Serra was born in 1940. He received the degree of mining engineering in 1962, and the Ph.D. degree in geostatistics in 1967. During this time, in cooperation with Georges Matheron, he laid the foundations of a new method called "mathematical morphology" (1964), the purpose of which was to describe quantitatively shapes and textures of natural phenomena, at micro and macro scales.

In 1967, he (with G. Matheron) founded the Centre de Morphologie Mathématique at the Paris School of Mines. He has been working in this framework as a Director of Research. He successively oriented mathematical morphology toward optical microscopy (in the 1970s), industrial control (in the 1980s), and multimedia (in the 1990s). In the last 15 years, his three major contributions to mathematics and physics include: morphological filtering, which is an alternative to Fourier analysis (in cooperation with G. Matheron, 1982–1987); the formulation of mathematical morphology in the convenient framework of complete lattices (in cooperation with G. Matheron, 1984–1988); and a theory for connectivity adapted to image analysis, 1993–2000. He holds several patents of devices for image processing. His main book is a two-volume treatise entitled *Image Analysis and Mathematical Morphology* (New York: Academic, 1982, 1988).

Dr. Serra was Vice President for Europe of the International Society for Stereology from 1979 to 1983. He founded the International Society for Mathematical Morphology in 1993, and was elected its first president. He has received various awards and titles, such as Doctor Honoris Causa of the University Autonoma of Barcelona, Spain, in 1993, and the first AFCET Award in 1988.